

Chapter 2

Background

Some background is necessary for understanding the concepts presented in this thesis. This chapter attempts to provide the reader with the information necessary to understand later chapters. Relevant references are included for the interested reader. The first section presents a brief discussion of the nature of short pulses. Section 2.2 addresses issues related to the linear and nonlinear propagation of these short pulses. In the final section, a brief history of pulse measurement techniques demonstrates the timeliness of these measurements and provides a motivation for the technique we have chosen.

2.1 Short Pulses

A light pulse can be described as a group of optical cycles under a pulse envelope. A short pulse in time necessarily has a broad spectral bandwidth as a result of the Fourier relationship between time and frequency. A shorter pulse requires a larger frequency bandwidth than a longer pulse. For a given pulse length in time, the minimum spectral bandwidth can be calculated using the time-bandwidth product. For a Gaussian pulse and using FWHM of intensity values of the time and spectral bandwidth, the minimum time bandwidth product is 0.441. Using rms values, the minimum time-bandwidth product for a Gaussian pulse is 0.5. Reference [4] gives a table of the minimum time-bandwidth products for a variety of common pulse shapes. Pulses with a

time-bandwidth product close to the minimum value are said to be “transform-limited”. A transform-limited, 100 fs pulse spectrally centered at 800 nm has a spectral FWHM of roughly 9.5 nm.

A short pulse can be described as a carrier frequency, ω_0 , and a complex Gaussian envelope of the form:

$$\mathcal{E}(t) = \exp(-at^2) \exp[i(\omega_0 t + bt^2)]. \quad (2.1)$$

In this equation, $\exp[i(\omega_0 t + bt^2)]$ is the time-varying phase shift of the sinusoidal signal within the Gaussian pulse. The total instantaneous phase is then

$$\Phi_{tot}(t) = \omega_0 t + bt^2.$$

The rate at which the total phase propagates forward in time is the instantaneous frequency and is defined as the derivative of the phase with respect to time:

$$\omega(t) \equiv \frac{d\Phi_{tot}(t)}{dt}.$$

For the Gaussian pulse in Eq. 2.1,

$$\omega(t) = \frac{d}{dt}(\omega_0 t + bt^2) = \omega_0 + 2bt. \quad (2.2)$$

If $b \neq 0$, then the instantaneous frequency varies linearly in time. In other words, the component frequencies of the pulse are ordered in increasing or decreasing fashion in time. Such a pulse is said to be chirped. The term “chirp” comes from the sound a bird makes when it chirps. In that case, acoustic frequencies increase or decrease with time. In Eq. 2.2, b is called the chirp parameter and provides a measure of the chirp of the pulse. The presence of chirp increases the time-bandwidth product of a pulse by a factor of $\sqrt{1 + (b/a)^2}$. Therefore, by propagating a chirped pulse through a medium such that the different frequencies travel at different speeds and the chirp is reduced or eliminated, the pulse can be compressed in time. Equation 2.2 also illustrates that

a linear frequency chirp (linear with respect to time) occurs as a quadratic term in the phase. This point will be relevant when examining data presented in later chapters of this thesis.

2.2 Short Pulse Propagation

As a pulse propagates, the velocity at which the carrier frequency travels through a dispersive medium is called the phase velocity. The phase velocity is determined by the propagation constant, k , evaluated at the carrier frequency. The propagation constant is given by $k = 2\pi n/\lambda_0$ where n is the index of refraction of the material. The velocity at which the envelope travels is called the group velocity. The group velocity is given by the first derivative with respect to frequency of the propagation constant. When the group velocity itself is frequency dependent, the component frequencies of the pulse travel at different velocities. This frequency dependent group velocity is known as group velocity dispersion (GVD). GVD leads to changes in pulse shape, such as compression or stretching in time, as a pulse propagates. GVD is given by the second derivative of the propagation constant with respect to frequency. Since k goes as n/λ_0 , a plot of n versus the free-space wavelength, λ_0 , reveals regions of positive and negative GVD. Positive or normal dispersion occurs at wavelengths where the curve is concave up – where the second derivative is positive. Downward curvature indicates regions of negative, or anomalous dispersion. At visible wavelengths, most common optical materials exhibit normal dispersion. With normal GVD, red-shifted frequencies travel faster than blue-shifted frequencies, leading to an upchirped pulse.

Propagation of an electromagnetic wave can be described by starting from Maxwell's

equations for a neutral, non-magnetic, dielectric medium:

$$\begin{aligned}\nabla \times \mathbf{E} &= \frac{-\mu_0 \partial \mathbf{H}}{\partial t} \\ \nabla \times \mathbf{H} &= \frac{\partial \mathbf{D}}{\partial t} \\ \nabla \cdot \mathbf{B} &= 0 \\ \nabla \cdot \mathbf{D} &= 0.\end{aligned}$$

For non-magnetic media,

$$\mathbf{B} = \mu_0 \mathbf{H}.$$

And the electric displacement, \mathbf{D} , is given by

$$\mathbf{D} = \epsilon_0 \mathbf{E} + \mathbf{P}.$$

\mathbf{P} represents the polarization, in units of electric dipole moment per unit volume, of the medium and is the only term in Maxwell's equations that relates directly to the medium. In the above equations, μ_0 is the permeability of free space, and ϵ_0 is the permittivity of free space. Taking the curl of $\nabla \times \mathbf{E}$ with

$$\begin{aligned}\frac{1}{\sqrt{\mu_0 \epsilon_0}} &= c \quad \text{and} \\ \nabla \cdot \mathbf{E} &= 0 \quad (\text{transverse waves})\end{aligned}$$

gives the one-dimensional inhomogeneous wave equation:

$$\nabla^2 \mathbf{E} - \frac{1}{c^2} \frac{\partial^2 \mathbf{E}}{\partial t^2} = \frac{1}{\epsilon_0 c^2} \frac{\partial^2 \mathbf{P}}{\partial t^2}. \quad (2.3)$$

If the polarization, \mathbf{P} , is linear in the applied field, then the propagation is linear. This linear response of the medium is simply the index of refraction. If the applied field is strong enough, \mathbf{P} can become nonlinear in the applied field. This is what is meant when one discusses nonlinear propagation. A good introduction to nonlinear optics can be found in Chapter 17 of Ref. [5]. A simplified description of some of the

basic concepts that will be important for understanding the work presented in this thesis follows.

\mathbf{P} can be expressed as a series expansion in the applied field:

$$\mathbf{P} = \chi_1 \epsilon_0 \mathbf{E} + \chi_2 \mathbf{E}^2 + \chi_3 \mathbf{E}^3 + \dots$$

In this expression, χ_n provides a measure of the strength of the linear or nonlinear process and is called the susceptibility. As is expected with a series expansion, higher order susceptibilities have decreasing strength. In other words, higher order nonlinearities require a stronger field to have any effect on the propagation. It is for this reason that nonlinear optical processes were largely inaccessible to researchers prior to the availability of lasers. Commercial femtosecond lasers now routinely produce pulses with peak intensities on the order of 10 GW/cm² or higher.

The second order nonlinearity, $\chi_2 \mathbf{E}^2$, is responsible for second-harmonic generation and optical parametric amplification among other things. Both of these effects arise from a transfer of energy between electromagnetic fields of different frequencies within the material such that

$$\omega_3 = \omega_1 + \omega_2.$$

Second-harmonic generation is a special case of this general expression, where $\omega_1 = \omega_2$. In this case, light at the fundamental frequency is converted to light at the second harmonic frequency: $\omega_3 = 2\omega_1$. In parametric amplification, the opposite effect occurs. Fundamental light at ω_3 causes the generation of light at ω_1 and ω_2 , where ω_1 and ω_2 are not necessarily equal. Second order nonlinearities only occur in non-centrosymmetric materials such as Beta-Barium Borate (BBO), Potassium Dihydrogen Phosphate (KDP) and Lithium Niobate. A list of the second order nonlinear coefficients of some commonly used crystals can be found in Ref. [6].

The third order nonlinearity is active in all materials, regardless of symmetry, and gives rise to some interesting effects, including four-wave mixing, Raman scatter-

ing, and the optical Kerr effect. Four-wave mixing includes all processes where one frequency is created from the combination of three other frequencies. For example, the situations $\omega_4 = \omega_1 + \omega_2 + \omega_3$, $\omega_4 = \omega_1 + \omega_2 - \omega_3$, $\omega_4 = -\omega_1 - \omega_2 + \omega_3$ etc. are all classified as four-wave mixing. Third-harmonic generation is a special case of four-wave mixing in which $\omega_1 = \omega_2 = \omega_3$, and $\omega_4 = 3\omega_1$. The Raman nonlinearity is also a version of four-wave mixing in which a molecule makes a transition between two states. Figure 2.1 illustrates this process. A pump photon excites the molecule into a higher energy virtual state from which the molecule immediately drops back down to either state 1 or state 2. Raman scattering occurs when the molecule ends up in a different state than it was initially such that $\omega_f = \omega_p - \omega_{1-2}$ (Stokes) or $\omega_f = \omega_p + \omega_{1-2}$ (anti-Stokes). In the preceding equations, ω_f represents the emitted frequency, ω_p represents the pump frequency, and ω_{1-2} represents the energy difference, expressed in terms of frequency, between states 1 and 2. Raman scattering can occur as either a spontaneous or stimulated process. Since at thermal equilibrium most molecules will initially be in the lower of states 1 and 2, more light will scatter into the lower frequency (Stokes) emission than into the higher frequency (anti-Stokes) emission. As a result, the Raman nonlinearity should result in a shifting of pulse frequencies to the red.

The optical Kerr effect is a result of anharmonic motion of bound electrons in the material and results in an intensity dependent refractive index. The index of refraction of the material is then described by $n = n_0 + n_2 I$ where n_0 is the linear index of refraction and $n_2 I$ is the intensity dependent nonlinear index of refraction. The optical Kerr effect is responsible for three important phenomena in nonlinear pulse propagation: self-phase modulation (SPM), self-focusing (SF), and self-steepening(SS).

Self-Phase Modulation In self-phase modulation, the time-varying index of refraction produces a time dependent phase modulation of the pulse and thereby contributes to spectral broadening of the pulse. Consider the propagation-induced phase of

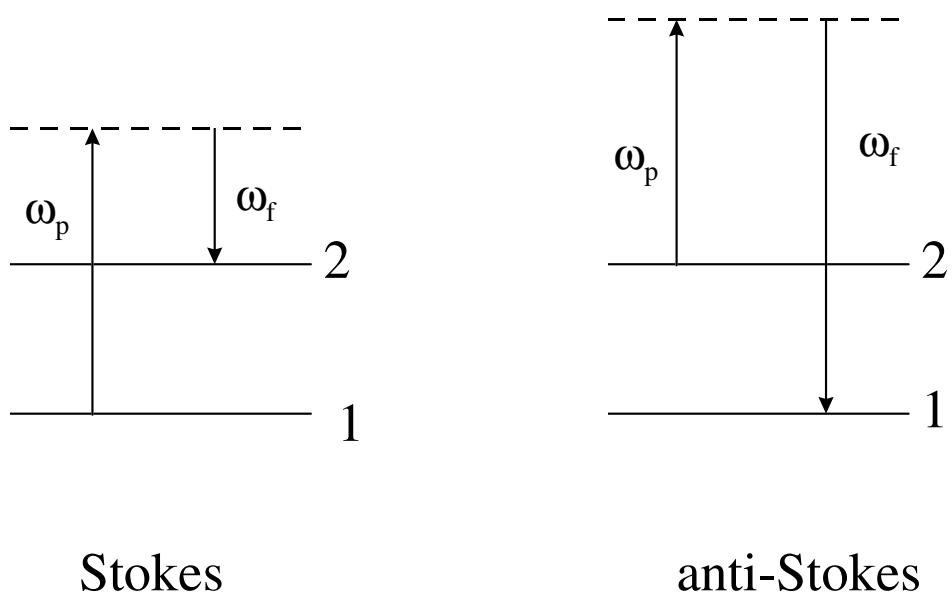


Figure 2.1: Schematic diagram of the Stokes and anti-Stokes Raman scattering processes.

a pulse:

$$\Phi(t) = \omega_0 t - kz$$

where k is the propagation constant, z is the propagation distance through the medium, and ω_0 is the center frequency of the pulse. For a medium of length L , the phase after propagation is given by:

$$\Phi(t) = \omega_0 t - \frac{2\pi n}{\lambda} L$$

where n is the total index of refraction given by $n = n_0 + n_2 I$. Now, the instantaneous frequency is the derivative of the phase with respect to time which is given by:

$$\frac{d\Phi}{dt} = \omega_0 - \frac{2\pi L}{\lambda} \frac{dn}{dt}$$

or

$$\frac{d\Phi}{dt} = \omega_0 - \frac{2\pi n_2 L}{\lambda} \frac{dI(t)}{dt}.$$

The instantaneous frequency, therefore, goes as the negative of the derivative of the intensity profile with respect to time. Assuming n_2 is positive, this leads to a lowering of frequencies on the leading edge of the optical pulse and an increase in frequencies at the trailing edge of the pulse. A pulse with a smooth Gaussian envelope will thus acquire a roughly linear frequency chirp across the central region of the pulse. This situation is illustrated in Fig. 2.2. Note that SPM is similar to GVD in that it produces a frequency chirp. However, SPM actually shifts some of the component frequencies of the pulse to new frequencies while GVD only rearranges the component frequencies.

Self-Focusing Self-focusing is a nonlinear effect that results in a spatial focusing of the beam as it propagates. SF is also a result of the optical Kerr effect. If n_2 is positive, then the higher intensity regions of the pulse experience a larger index of

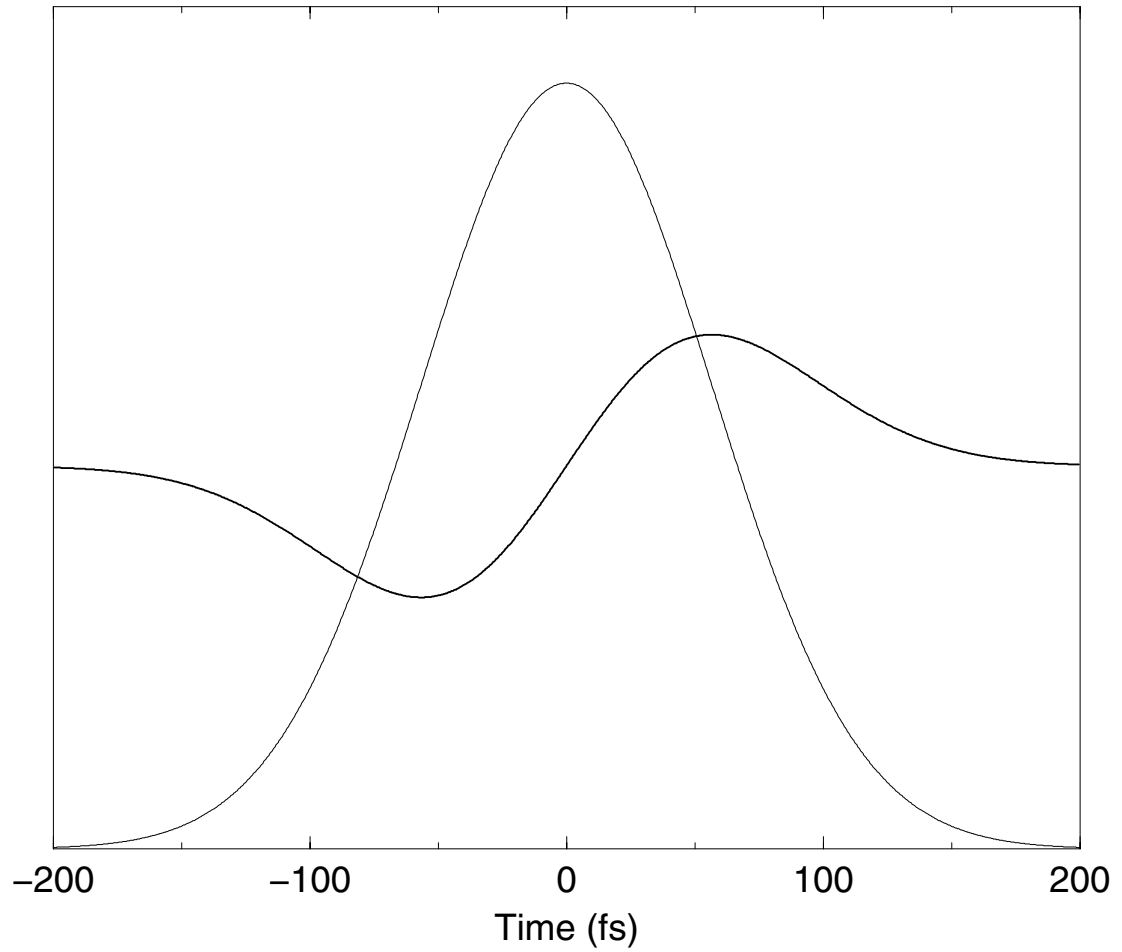


Figure 2.2: A Gaussian function and the negative derivative of that Gaussian. The derivative illustrates the change in frequency a Gaussian pulse experiences as a result of SPM.

refraction than the lower intensity wings of the pulse. In this way, the pulse transforms the medium into a weak positive lens. As the pulse is focused, the center becomes more intense leading to a higher index of refraction and an even stronger positive lens. In this manner, self-focusing can become a large effect very quickly. This type of SF is known as whole beam self-focusing. In similar fashion, any small spike or ripple on the pulse envelope can be magnified greatly and seriously distort the original pulse shape. This type of SF is known as small-scale self-focusing. Either type of SF can be catastrophic in an optical system. The high intensities present in the focusing pulse can be sufficient to damage most optical elements. Two important quantities associated with SF are the critical power for self-focusing, given by $P_{crit} = (0.61\lambda)^2\pi/(8n_0n_2)$, and the self-focusing distance, $z_f = w_0 \sqrt{n_0/(n_2I)}$ [7].

Self-Steepening Self-steepening refers to the steepening of one of the pulse edges in the temporal domain during propagation. This pulse edge deformation is accompanied by an asymmetry in the pulse spectrum [8]. SS occurs as a result of an intensity dependent group velocity. The group velocity decreases with increasing intensity as a result of the intensity dependent index of refraction. The leading and trailing edges of the pulse therefore travel faster than the central portion, leading to a steepening of the trailing edge of the pulse in the temporal domain.

Nonlinear Schrödinger Equation The basic equation describing propagation in a weakly nonlinear medium is the one-dimensional nonlinear Schrödinger equation (NLSE):

$$\frac{\partial \mathcal{E}}{\partial z} + i \frac{k''}{2} \frac{\partial^2 \mathcal{E}}{\partial t^2} - i \frac{2\pi n_2}{\lambda} |\mathcal{E}|^2 \mathcal{E} = 0. \quad (2.4)$$

In this equation, \mathcal{E} is the slowly varying complex amplitude of the field in the reference frame moving at the group velocity. GVD is determined by k'' , and the third term gives the optical Kerr effect. The field is normalized such that $|\mathcal{E}|^2$ is the intensity in units of

W/cm².

The above mentioned linear and nonlinear effects come into play in various aspects of the research presented in this thesis. Many of these effects play a crucial role in the generation of ultrashort pulses. Second-harmonic generation is the nonlinearity on which the most often used measurement technique in this thesis is based. Linear and nonlinear propagation effects are important in the propagation experiments performed throughout this thesis. The preceding discussion of these effects should provide the reader with the background necessary to understand the science presented in this thesis.

2.3 History of Short Pulse Measurement

To interrogate the processes involved in propagation of femtosecond pulses, it is first necessary to be able to measure the pulses themselves. By measuring a pulse before and after traversing the material of interest, one can infer valuable information regarding the materials parameters. Changes in the pulse spectrum, intensity profile, and phase are all important. Also, for numerically modeling pulse propagation, an accurate determination of the peak intensity of the pulse is required. This section provides a brief history of pulse measurement techniques and a description of the full-field techniques available for pulse measurement today.

Acquiring the spectrum of a short pulse is not a difficult task provided one is careful not to distort the pulse spectrum during the measurement. Measuring the temporal duration of the pulse, however, is a more daunting task because measuring a short pulse requires an event that is even shorter. Autocorrelation techniques provide an obvious solution to this quandary because they use the pulse to measure itself. A 1974 publication by Bradley and New [9] provides an excellent overview of the measurement techniques first used to measure short pulses such as linear and nonlinear autocorrelation.

Autocorrelation works by dividing the pulse to be measured into two replicas and then interacting these two replicas over a range of delays to produce a signal. Linear correlation relies on measuring interference fringes between the two pulses while non-linear correlation techniques involve overlapping the two pulses in a nonlinear medium to produce a signal. An example is overlapping the two pulses in a second-harmonic generating crystal. In this case, the signal produced is given by the second-order correlation function: $\int I(t)I(t + \tau)dt$. This signal can be produced in the presence of a constant background or in a background-free configuration. Because a signal will only be observed or enhanced above background while the two pulses are overlapped, these methods give the user some insight into the duration of the pulse. The absolute length of the pulse, however, cannot be obtained. To place any value on the length of the pulse one must first assume a pulse shape. Often a pulse is assumed to be Gaussian or hyperbolic secant squared in shape. If both the autocorrelation and the spectrum are available, the time-bandwidth product gives some insight into phase of the pulse insofar as it confirms the presence or absence of chirp.

Autocorrelations have been performed in a variety of configurations. Because one arm of the autocorrelator is scanned to produce signal over a range of delays, early experiments with short pulses were necessarily multi-shot experiments. In an effort to measure the duration of a single pulse, and not a time average length, researchers turned to performing autocorrelations in laser dyes, observing two photon fluorescence as the signal. Counter propagating pulses led to single shot measurements. The technique, however, did not lend itself to background free configurations and the signal to noise ratio often led to unreliable information. Streak cameras were employed to measure pulses of picosecond and longer duration. Early work also employed ultrafast shutters, where one pulse is used as a gate function, allowing the signal to pass through a Kerr or saturable absorber medium. Borrowing from the field of acoustics in 1971, Treacy first applied the concept of a spectrogram to the optical regime [10]. A spectrogram

is a two-dimensional representation of the pulse as a function of time and frequency. Treacy was, however, unable to retrieve the full intensity and phase of the pulse. Third and higher correlation experiments were also performed in the first attempts to uncover some phase information as well.

As short pulse technology progressed, techniques were developed that could better measure the intensity profile of a femtosecond pulse. Techniques based on four-wave mixing, third-harmonic generation, or a combination of sum- and difference-frequency generation were proposed and implemented to measure complicated or asymmetric intensity profiles [11, 12]. These methods worked well, however they could only measure pulses in the visible. A much later optical Kerr shutter technique allowed measurement of pulse asymmetry and structure of pulses in the UV [13].

Other methods were designed to measure the presence of chirp [14, 15, 16]. These methods, however, were limited either because they used a streak camera and thus were not useful for very short pulses, or they could only resolve whether or not a pulse was chirped. In 1991 Albrecht *et al.* developed a method based on two-photon absorption to characterize the phase function of a pulse up to the fourth order. A separate technique, however, was required to gain any information about the temporal shape or duration of the pulse [17]. Later, Le Blanc and Sauerbrey developed a technique that avoided the use of a nonlinear detector, thus allowing measurement of pulses from the ultraviolet to the XUV. Results of this technique, however, were difficult to interpret, and the technique was only capable of resolving phase shifts of π or larger [18].

As early as 1985, the first methods to simultaneously measure both the amplitude and phase of femtosecond pulses appeared. The first successful technique was implemented by Diels *et al.* [4]. Theirs is something of a brute force method. The idea is to measure the pulse spectrum, the intensity autocorrelation, and the interferometric autocorrelation and then iteratively fit a pulse to the three results until the process converges to the one pulse that could have produced all three. This technique still requires some

previous knowledge or a reasonable estimate of the functional dependence of the pulse and therefore isn't particularly useful for complicated pulse shapes or modulations. Also, there has been no discussion of the uniqueness of the solution. Naganuma presented a more rigorous variation on this theme and demonstrated that a measurement of the interferometric intensity autocorrelation and the interferogram of the fundamental is mathematically sufficient to reconstruct the pulse with ambiguity only in the direction of time [19]. Later work resolves the time ambiguity by making measurements before and after propagation through a piece of glass [20].

Another method relies on time domain interferometry, but requires a flat phase reference pulse [21]. Diels later introduced a more elegant technique where one applies a known reversible transformation to the pulse to be measured so as to stretch out the signal in time [22]. This pulse is then characterized by interferometric cross correlation with the short version of itself. The fully characterized long pulse is numerically transformed back. In practice this reversible transformation might be propagation through a piece of glass. Of course, this method assumes a full understanding of the processes involved in the propagation as well as accurate parameters associated with these processes. If the pulse is of low enough peak intensity, this assumption is not an unreasonable one.

Each of the preceding measurement techniques for resolving the intensity and phase of a pulse involves measurements in the time domain, in the spectral domain, or in both. The real breakthrough came, however, with techniques involving measurements in a combined temporal-spectral domain. In one of the first optical temporal-spectral measurements, Treacy directly measured chirp in a pulse using time-resolved spectroscopy [23]. Dynamic spectrograms have also been applied to the determination of the presence of temporal asymmetry and chirp in compressed pulses [24]. In fact, it was a spectrographic technique that facilitated the compression of pulses to 6 fs for the first time. Treacy had predicted that cubic phase would be the limiting factor in produc-

ing short pulses [25]. The record in 1987 was 8 fs, produced by grating compression of a pulse spectrally broadened by SPM in a single mode optical fiber [26]. Fork *et al.* produced 8 fs pulses using this method. Then, by mixing six different spectral regions of the compressed pulse with an unbroadened pulse from the amplifier and upconverting each, he was able to measure the relative delay experienced by each frequency component. In this manner he could see that the 8 fs pulse had a residual cubic phase term. By adding a prism pair and adjusting the distances between prisms and gratings, he was able to eliminate both cubic and quadratic phase and achieve 6 fs pulses [2]. Fork's clever measurement technique formed the basis of the first spectrographic pulse measurement techniques.

In 1991 Chilla and Martinez published a combined spectral-temporal pulse measurement technique based on Fork's work that provided the first direct measurement of amplitude and phase [27]. The method first filters the pulse to be measured in frequency, selecting a narrow frequency range. This spectral piece is then cross correlated with a reference pulse to measure delay. By moving the filter and thereby selecting different frequency regions, the derivative of the phase can be found as a function of frequency. An integral yields spectral phase. This information, in conjunction with the power spectrum, gives the spectral amplitude and phase of the pulse. The temporal amplitude and phase are given by Fourier transform. This technique was termed frequency domain phase measurement or FDPM [28].

A similar technique upconverts the pulse to be measured with a spectrally narrow reference pulse [29]. At each value of delay, the spectrum is recorded. The delay at which each wavelength exhibits an intensity maximum is related to the phase. The reference pulse is narrow so that each upconverted sum-frequency corresponds to nearly one frequency component of the pulse to be measured. A rigorous development of the theory behind this technique was presented. This method was experimentally demonstrated to measure only the phase but, in theory, it has sufficient information to

determine the full complex pulse field [30].

Both of the immediately preceding techniques are members of a larger class of techniques whose members are each referred to as a STRUT: spectrally and temporally resolved upconversion technique.

Kane and Trebino introduced a technique similar to FDPM, known as frequency-resolved optical gating or FROG [31]. Instead of temporally resolving spectral slices of a pulse, however, FROG spectrally resolves temporal slices of a pulse. The temporal gating can be accomplished in several ways, but all methods rely on spectrally resolving the signal from an autocorrelation performed in an instantaneously responding nonlinear medium. This measurement yields the spectrogram of the pulse. The intensity and phase of the pulse is then retrieved by means of an iterative two-dimensional phase retrieval algorithm that requires no assumptions about the pulse. The retrieved field has been shown to be essentially unique [31]. The advantage of FROG over the Fourier filtering method of Chilla and Martinez is that it is experimentally simpler and can be extended to a single shot technique. More about the FROG technique can be found in Chapter 3.

Nearly two years after the introduction of FROG, a new technique was introduced by B.S. Prade *et al.* This method is experimentally simpler than FROG and can also be performed in a single shot. The method makes two measurements of the power spectrum of the pulse: one before and one after propagation through a known Kerr medium where the spectrum acquires a complicated fringe structure. A retrieval algorithm starts with an initial guess for the pulse and numerically forward and backward propagates the pulse, replacing the spectrum with the corresponding measured values between each step, until the algorithm converges to a single input that is consistent with both measurements. Uniqueness of the solution is not proven, but the technique has been demonstrated to be robust by introducing known phase distortions on a pulse and then performing the measurement. The technique also provides a measure of the

peak intensity of the pulse assuming the nonlinear index of refraction of the material is known accurately.

In 1995 a method was described that directly measures spectral phase, thus eliminating the need for a retrieval algorithm and the worries of uniqueness [32]. This method, which is essentially the same as a technique developed in femtosecond pulse shaping experiments [33], is called direct optical spectral phase measurement (DOSPM). In DOSPM, the pulse to be measured is spectrally dispersed with a grating. A V-shaped filter then selects two narrow spectral components, one of which is located at the center wavelength. Temporal beat patterns are then measured by cross correlation with a nearly transform limited reference pulse. Phase differences appear as a delay of the center peak of the beat pattern. By varying the height of the V-shaped filter, and thus the spectral component selected, to both positive and negative offsets, the frequency dependent phase can be directly determined. This method, however, gives no information about the amplitude of the pulse. Both DOSPM and the second-harmonic generation form of FROG have been shown to measure phase distortions to within 5% accuracy [34]. DOSPM was later modified to employ a multi-slit arrangement [35]. This arrangement allows for single shot measurement and is capable of measuring more complicated or discontinuous phase profiles.

The preceding techniques are those that were available at the time the investigations presented in this thesis began. For completeness, I mention here other pulse measurement techniques that have since been developed.

Two additional STRUTs have been developed. The first method again overlaps a spectrally narrow (1.5 nm) reference pulse with the pulse to be measured in a nonlinear crystal to produce an upconversion signal, but it does so in a single shot geometry [36]. The measurement yields a real time group delay spectrogram from which amplitude and phase can be determined using a rapid retrieval algorithm. This method boasts close to real time phase and amplitude displays. It also employs a second-order

nonlinear process and is therefore useful for weak signals. The second method, temporal analysis of spectral components (TASC), is experimentally the same method as FDPM except that it uses a wider slit when selecting spectral components [37]. FDPM is limited to measuring simple phase structures because it discards information on the full temporal dependence of each spectral piece. TASC selects broad enough spectral components that the temporal profile is not determined by the spectral mask. TASC is also a second order technique capable of measuring weak pulses. The method boasts intuitive spectrograms and no time direction ambiguity.

Two methods have recently been introduced to measure not only amplitude and phase but also peak intensity. One technique provides a measurement in the focal region of a pulse and is based on measuring two far-field intensity patterns: one with and one without a known nonlinear material located in the focal spot. This technique was dubbed BRIEFING or beam reconstruction by iteration of an e-field with an induced nonlinearity gauge [38]. A second method involves triple correlation and involves no assumptions about the analytic form of the pulse and uses no iterative algorithms [39].

In the past, femtosecond nonlinear pulse propagation has been studied by spectral observations [40, 41], autocorrelations [42], and cross correlations [43]. Information about the spatial effects of nonlinear pulse propagation have been obtained using the z-scan technique [44, 45]. Although these techniques provide important information, they generally require assumptions about the pulse and they do not provide a measure of the phase. Among the full-field techniques, FROG has emerged as a powerful, robust, and widely-used pulse diagnostic. Although FROG has primarily functioned as a diagnostic technique, it also holds value as a tool for measuring nonlinear materials properties as will be demonstrated in the following chapters.